

# **PROJECT REPORT**

**On**

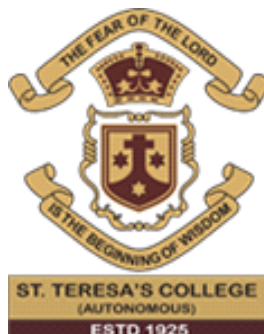
**ZnO-GO COMPOSITES: AN EFFICIENT PHOTOCATALYST  
FOR DEGRADATION OF METHYLENE BLUE**

Submitted by

**ATHEENA RANSOM ARUJA (AB21CHE002)  
JYOTHI PRAKASAN (AB21CHE018)  
SANIA JOSEPH (AB21CHE025)  
SHIFANA E N. (AB21CHE027)**

*In partial fulfilment for the award of the*

**Bachelor's Degree in Chemistry**



**DEPARTMENT OF CHEMISTRY AND CENTRE FOR RESEARCH**

**ST. TERESA'S COLLEGE (AUTONOMOUS)  
ERNAKULAM**

**2023-2024**

DEPARTMENT OF CHEMISTRY AND CENTRE FOR RESEARCH

ST. TERESA'S COLLEGE (AUTONOMOUS)

ERNAKULAM



**B.Sc. CHEMISTRY PROJECT REPORT**

Name : ATHEENA RANSOM ARUJA  
Register Number : AB21CHE002  
Year of Work : 2023-2024

This is to certify that the project “**ZnO-GO COMPOSITES: AN EFFICIENT PHOTOCATALYST FOR DEGRADATION OF METHYLENE BLUE**” is the work done by **ATHEENA RANSOM ARUJA**.

**Dr. Saritha Chandran A.**  
Head of the Department

**Dr. Saritha Chandran A.**  
Staff-member in charge

Submitted to the Examination of Bachelor's Degree in Chemistry

Date: 11/5/24.....

Examiners: Dr. Ajith James Jose, SB College, Chayyur  
Dr. Nisha P. P. TRISA

DEPARTMENT OF CHEMISTRY AND CENTRE FOR RESEARCH

ST. TERESA'S COLLEGE (AUTONOMOUS)

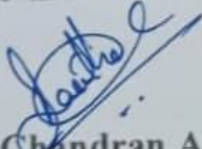
ERNAKULAM

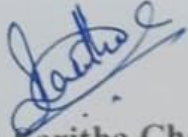


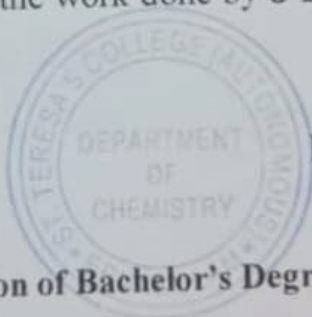
B.Sc. CHEMISTRY PROJECT REPORT

Name : JYOTHI PRAKASAN  
Register Number : AB21CHE018  
Year of Work : 2023-2024

This is to certify that the project "ZnO-GO COMPOSITES: AN EFFICIENT PHOTOCATALYST FOR DEGRADATION OF METHYLENE BLUE" is the work done by JYOTHI PRAKASAN.

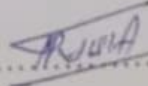
  
Dr. Saritha Chandran A.  
Head of the Department

  
Dr. Saritha Chandran A.  
Staff-member in charge



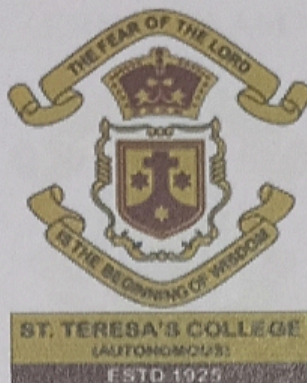
Submitted to the Examination of Bachelor's Degree in Chemistry

Date: 4/5/24

Examiners: Dr. Ajith James Jase, SB College Chyay Jase  
Dr. Nisha T. P. 

DEPARTMENT OF CHEMISTRY AND CENTRE FOR RESEARCH

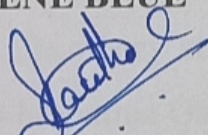
ST. TERESA'S COLLEGE (AUTONOMOUS)  
ERNAKULAM

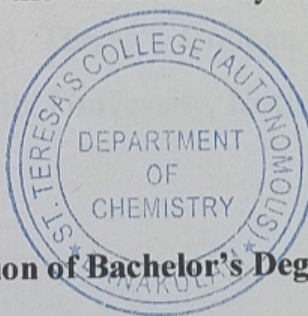


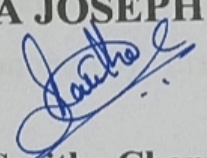
B.Sc. CHEMISTRY PROJECT REPORT

Name : SANIA JOSEPH  
Register Number : AB21CHE025  
Year of Work : 2023-2024

This is to certify that the project “ZnO-GO COMPOSITES: AN EFFICIENT PHOTOCATALYST FOR DEGRADATION OF METHYLENE BLUE” is the work done by SANIA JOSEPH .

  
Dr. Saritha Chandran A.  
Head of the Department

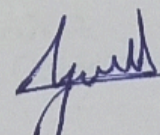
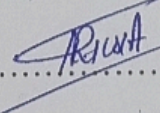


  
Dr. Saritha Chandran A.  
Staff-member in charge

Submitted to the Examination of Bachelor's Degree in Chemistry

Date: ... 4/5/2024 .....

Examiners: ...

Dr. Ajith James Jose, SB College Chygy   
Dr. Nisha P.P. 

DEPARTMENT OF CHEMISTRY AND CENTRE FOR RESEARCH

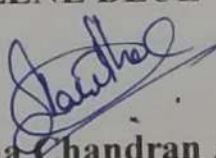
ST. TERESA'S COLLEGE (AUTONOMOUS)  
ERNAKULAM

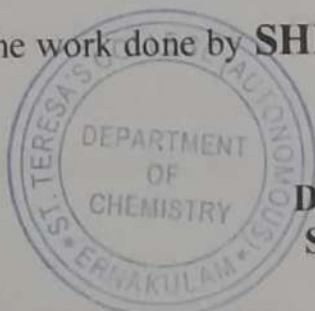


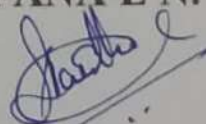
B.Sc. CHEMISTRY PROJECT REPORT

Name : SHIFANA E N.  
Register Number : AB21CHE027  
Year of Work : 2023-2024

This is to certify that the project "ZnO-GO COMPOSITES: AN EFFICIENT PHOTOCATALYST FOR DEGRADATION OF METHYLENE BLUE" is the work done by SHIFANA E N.

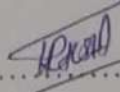
  
Dr. Saritha Chandran A.  
Head of the Department



  
Dr. Saritha Chandran A.  
Staff-member in charge

Submitted to the Examination of Bachelor's Degree in Chemistry

Date: 4/5/24

Examiners: Dr. Ajith James Jave, S.B. College, Chydyndil  
: Dr. Nisha P.P. 

**DEPARTMENT OF CHEMISTRY AND CENTRE FOR RESEARCH**

**ST. TERESA'S COLLEGE (AUTONOMOUS)**

**ERNAKULAM**



**CERTIFICATE**

This is to certify that the project work entitled “**ZnO-GO COMPOSITES: AN EFFICIENT PHOTOCATALYST FOR DEGRADATION OF METHYLENE BLUE**” is the work done by **ATHEENA RANSOM ARUJA, JYOTHI PRAKASAN, SANIA JOSEPH, SHIFANA E N.** under my guidance in the partial fulfilment of the award of the Degree of Bachelor of Science in Chemistry at St. Teresa's College (Autonomous), Ernakulam affiliated to Mahatma Gandhi University, Kottayam.

Dr. SARITHA CHANDRAN A.  
Project Guide

## **DECLARATION**

I hereby declare that the project work entitled “**ZnO-GO COMPOSITES: AN EFFICIENT PHOTOCATALYST FOR DEGRADATION OF METHYLENE BLUE**” submitted to Department of Chemistry and Centre for Research, St. Teresa’s College (Autonomous) affiliated to Mahatma Gandhi University, Kottayam, is a record of an original work done by me under the guidance of **Dr. SARITHA CHANDRAN A., HEAD OF THE DEPARTMENT**, Department of Chemistry and Centre for Research, St. Teresa’s College (Autonomous), Ernakulam and this project work is submitted in the partial fulfilment of the requirements for the award of the Degree of Bachelor of Science in Chemistry.

ATHEENA RANSOM ARUJA

JYOTHI PRAKASAN

SANIA JOSEPH

SHIFANA E N.

## *Acknowledgements*

---

The success and the final outcome of this project required a lot of guidance and assistance from many people and we are extremely fortunate to have got this all along the completion of our project work. We hereby take this opportunity to acknowledge all the people who kept us forward in successfully completing this project. Above all, we express our deep sense of gratitude to God Almighty, for the completion of the work successfully, and his unlimited blessings throughout our life. We express our gratitude to our respected director, Rev. Sr. Dr. Vinitha CSST, St. Teresa's College and our principal Dr. Alphonsa Vijaya Joseph, St. Teresa's College Ernakulam, and the management for providing us the necessary facilities to successfully carry out our work. We respect and thank our project guide Dr. Saritha Chandran. A., Head of the Department of Chemistry, St. Teresa's College, for the inspiring guidance, scientific freedom, constant encouragement and cordial affection throughout the course of our study and research. We are thankful and fortunate enough to get constant encouragement, and remarkable suggestions throughout the project work from all the teaching staffs of our department. Also we would like to extend our sincere esteems to all staffs in laboratory for their timely support. We also express our heartfelt thanks to our parents for their valuable support and prayers. Finally, we would like to thank everybody who in their own way contributed in the successful realizations of the project.

ATHEENA RANSOM ARUJA

JYOTHI PRAKASAN

SANIA JOSEPH

SHIFANA E N.

## *Contents*

---

<b>Chapter 1 Introduction</b>	<b>1</b>
1.1 Nanotechnology	3
1.1.1 Definition and overview	3
1.1.2 Significance in contemporary research	4
1.2 Nanoparticles	4
1.2.1 Classification	5
1.2.2 Synthesis of nanoparticles	5
1.2.3 Uses of nanoparticles	6
1.3 Zinc oxide nanoparticle	8
1.3.1 Uses	9
1.3.2 Green synthesis	10
1.4 Graphene oxide	12
1.4.1 Structure	13
1.4.2 Properties	14
1.4.3 Uses	15
1.4.4 Synthesis	17
1.5 ZnO – GO nanocomposite	18
1.5.1 Properties	18
1.5.2 Synthesis	19
1.6 Photocatalytic activity of ZnO -GO composite	19
1.7 Application of ZnO- GO composite in literature	20
1.8 Objective	21

---

<b>Chapter 2 Materials and Methods</b>	<b>22</b>
2.1 Materials	22
2.1.1 Zinc nitrate	22
2.1.2 Graphite Powder	22
2.1.3 Hydrogen peroxide	22
2.1.4 Sulphuric acid	22
2.1.5 Potassium permanganate	22
2.1.6 Ethanol	22
2.2 Experimental methods	23
2.2.1 Green synthesis of zinc oxide nanoparticles	23
2.2.2 Synthesis of graphene oxide particle	24
2.2.3 Synthesis of ZnO -GO nanocomposite	24
2.2.4 Photodegradation of methylene blue	25
2.3 Characterization	26
2.3.1 X-ray diffraction (XRD)	26
2.3.2 Fourier transform infrared (FT-IR) spectroscopy	27
2.3.3 Transmission electron microscopy (TEM)	28
2.3.4 UV- visible spectroscopy	29
<b>Chapter 3 Results and Discussion</b>	<b>30</b>
3.1 Characterization of Zinc oxide	30
3.1.1 X-ray diffraction (XRD)	30
3.1.2 Fourier transform infrared (FT-IR) spectroscopy	34
3.1.3 Transmission electron microscopy (TEM)	35
3.2 Characterization of graphene oxide	35
3.2.1 X-ray diffraction (XRD)	35
3.2.2 Fourier transform infrared (FT-IR) spectroscopy	38

## *Contents*

---

3.2.3 Transmission electron microscopy (TEM)	40
3.3 Characterization of ZnO -GO nanocomposite	41
3.3.1 X-ray diffraction (XRD)	41
3.3.2 Fourier transform infrared (FT-IR) spectroscopy	45
3.3.1 Transmission electron microscopy (TEM)	45
3.4 Photo degradation of MB dye	46
3.4.1 UV- visible spectroscopy	46

<b>Chapter 4 Conclusions</b>	<b>48</b>
<b>References</b>	<b>49</b>

# Chapter 1

## Introduction

The wonders of nanomaterials are not unknown to us. The beauty of the butterfly wings and the spider web, has left us all in awe. Nanoparticles that occur naturally can be found in biological matter (such as viruses) fine sand and dust, volcanic ash and ocean spray. The diversity of synthetic nanoparticles is on par with that of their naturally occurring counterparts, if not greater. Stronger, lighter, cleaner, and "smarter" surfaces and systems can be made possible with the help of nanoparticles. Nanoparticles, usually less than 100 nanometers in size differ from bulk materials in their specific physical and chemical properties on account of their extremely small size. The quality and quantity of the synthesized nanoparticles are significantly influenced by a number of factors such as the synthesis method, temperature, pressure, time, particle size, pore size, environment and proximity<sup>1</sup>. However, because of the small particle diameter, the material can reach homogeneous equilibrium with respect to diffusion quickly as a whole. It has been discovered that variables like concentration, pH, and anions can directly have an impact on the size and stability of nanoparticles<sup>2</sup>.

Both ZnO and GO has been among the foremost nanoparticles to be extensively studied due to the unique properties possessed by them. ZnO is known for its powerful semiconducting, optical, and antibacterial properties, whereas GO provides excellent mechanical strength, larger surface area, and exhibits electronic properties. When these two materials

are combined at the nanoscale, the nanocomposites of ZnO-GO exhibits enhanced properties such as improved photocatalytic activity, electrical conductivity, and stability. These nanocomposites have potential applications in various fields, including electronics, sensors, photovoltaics, biomedical devices and among various other sectors.

The breakthrough of industrialization has brought massive changes all around, even in the environment. The development of industries and the large amounts of pollutants they generate such as oils, dyes, inorganic materials, organic solvents etc. that were released into water sources has led to a major issue of water pollution. The release of these contaminants into water supplies causes a shortage of clean, fresh water which is essential for the survival of the world's population. As a result, water pollution remains to be a cause of major concern for the society<sup>3</sup>.

Generally speaking, pigments and dyes released from industries pose a risk to human health and the environment. These environmentally harmful compounds can induce severe respiratory tract irritation, dermatitis, ulceration of the skin and mucous membranes, nasal septal perforation, and vomiting when consumed. They can also cause hemorrhage and acute diarrhea. Methylene blue (MB), a thiazine dye has several uses in analytical chemistry, biology, and even in medicine. But MB can be potentially hazardous to humans as it can cause fatal serotonin toxicity beyond a certain dose<sup>4,5</sup>. Apart from this, the effluents of industries containing MB can adversely affect the nitrifying bacteria, fishes and other aquatic lives. Because of the potential consequences on the environment and human health, the degradation of organic dyes from wastewater is of dire need in terms of environmental safety and has gained significant attention in recent

years. But efficient and economical color removal techniques are sometimes lacking in traditional approaches. This has eventually led to a notable increase in interest in cutting-edge materials and technology for the efficient degradation of dyes from aqueous solutions.

ZnO and GO nanoparticles have attracted interest among the developing materials due to their special qualities and combined synergistic effects. No nanoparticles are well known for their photocatalytic qualities, which allow them to efficiently degrade organic contaminants by producing reactive oxygen species when exposed to light. On the other hand, GO has a high adsorption capacity and can improve semiconductor materials like ZnO's photocatalytic efficiency. ZnO-GO nanoparticles gives the best qualities of both materials, offer a viable way to improve dye degradation when incorporated into a composite structure.

The preparation, characterization, and use of ZnO and GO nanoparticles for the degradation of MB organic dye are explored in this paper.

## **1.1 NANOTECHNOLOGY**

### **1.1.1 Definition and Overview**

With its use in science and technology to create nano-particles at the nanoscale level, nanotechnology is emerging as a quickly expanding area. New biocidal agents have been developed as a result of recent advancements in nanotechnology, specifically the capacity to create highly ordered nanoparticles of any size or shape. The term "a wonder of modern medicine" refers to nanomaterials. The scientific field of nanotechnology is diverse and rapidly developing. Unique structural, optical, and electrical features are provided by nanoscale particles that are not possible with single molecules or bulk substances. Because of their unique characteristics, which

include optical, magnetic, electrical, and catalytic activity, metal and metal oxide nanoparticles have piqued curiosity. A number of nanoparticle/biological interfaces have been formed as a result of nanoparticle contact with biological materials. These interfaces rely on both dynamic biophysicochemical interactions and colloidal forces. New nanomaterials with regulated size, shape, surface chemistry, roughness, and surface coatings are created as a result of these interactions. The synthesis of nanoparticles using plants is a revolutionary approach that offers a more economical and sustainable option than chemical and physical synthesis. Furthermore, the use of plants for large-scale synthesis can be readily expanded without the need for hazardous chemicals or extremely high pressures, temperatures, or energy. When a particle's size, dispersion, and shape diminish, nanoparticles have a larger surface area to volume ratio.

### **1.1.2 Significance in Contemporary Research**

Contemporary nanotechnology research holds immense significance across various fields. It enables advancements in medicine, materials science, electronics, and environmental sustainability. Nanoscale materials and devices offer unprecedented control at the atomic and molecular levels, fostering innovations like targeted drug delivery, efficient energy storage, and high-performance electronics. The potential for breakthroughs in diverse applications underscores nanotechnology's pivotal role in shaping the future of science and technology.

## **1.2 NANOPARTICLES**

The size of nanoparticles ranges from one to one hundred nanometers (nm). We refer to organic compounds that coat inorganic nanoparticles as passivating agents, capping and surface ligands, or stabilizers. A particle is defined in nanotechnology as a small entity that exhibits unit behavior in

terms of transport and characteristics. Depending on their diameter, particles are further categorized.

### 1.2.1 Classification

Nanomaterials have extremely small size, having at least one dimension of 100 nm or less. Nanomaterials can be nanoscale in one dimension (surface films), two dimensions (strands of fibers), or three dimensions (particles). They can exist in single, fused, aggregated or agglomerated forms with spherical, tubular, and irregular shapes. Common types of nanomaterials include nanotubes, dendrimers, quantum dots and fullerenes.

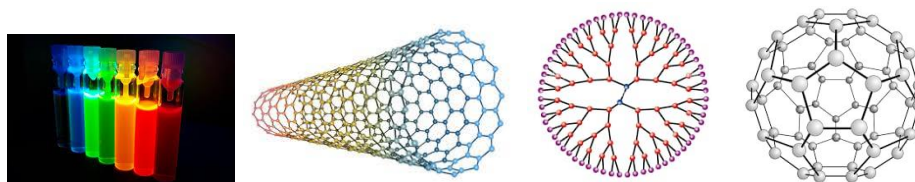


*Fig 1.1 Quantum dots, Carbon nanotubes, Dendrimers, fullerenes*

### 1.2.2 Synthesis of nanoparticles

The goal of any synthetic method for synthesis of nanomaterials is to yield a material that exhibits properties that are a result of their characteristic length scale being in the nanometer range (1 – 100 nm). Accordingly, the synthetic method should exhibit control of size in this range so that one property or another can be attained. Often the methods are divided into two main types, "bottom up" and "top down".

#### TOP - DOWN METHOD

Top-down methods adopt some 'force' (e.g., mechanical force, laser) to break bulk materials into nanoparticles. A popular method involves mechanical break apart bulk materials into nanomaterials is 'ball milling'.

Besides, nanoparticles can also be made by laser ablation which apply short pulse lasers (e. g. femtosecond laser) in order to vaporize a solid target.

#### **BOTTOM-UP METHOD**

Atoms or molecules can be assembled into nanostructured arrays using bottom-up techniques. These techniques can use gases, liquids, or solids as their raw material sources. The latter need to be disassembled in some way before being incorporated onto a nanostructure .

There are two main types of bottom-up methods:

- i) controlled
- ii) chaotic

- i) Elevating the component atoms or molecules to a chaotic state and then abruptly altering the environment to make that state unstable are the two steps involved in chaotic processes. Products arise primarily from the ensuring kinetics through the deft adjustment of numerous parameters.
- ii) In controlled processes, the constituent atoms or molecules are delivered to the site(s) of nanoparticle formation in a controlled way, allowing the nanoparticle to grow to the desired sizes.

#### **1.2.3 Uses of nanoparticles**

- ❖ The ZnO-GO nanocomposites' enhanced optical characteristics render them appropriate for use in photocatalytic and UV-Vis optoelectronics applications.
- ❖ Electronics, energy storage, (bio)sensors, biomedical applications, supercapacitors, membranes, catalysts, and water purification are just a few uses for reduced graphene oxide.

- ❖ Zinc oxide nanoparticles are widely used in nanomedicine, drug delivery, gene delivery, biological sensing, and biological labeling.
- ❖ Since graphene oxide-based nanocomposite materials have high surface areas, excellent mechanical strength, and can adapt to different functional groups, they have been widely used in the treatment of water and wastewater containing heavy metal ions and dye pollutants.
- ❖ Making lightweight sensors with nanocomposites.
- ❖ The nanotube spacing determines how well an electrical conductivity of a polymer-nanotube nanocomposite is conducted.  
Because of this characteristic, polymer-nanotube nanocomposite patches on windmill blades can function as stress sensors
- ❖ Using nanocomposites to make flexible batteries: A nanocomposite of cellulosic materials and nanotubes could be used to make a conductive paper.
- ❖ Enzyme nano-bioengineering aims to facilitate the conversion of cellulose found in corn stalks, wood chips, and unfertilized perennial grasses etc., into fuel-grade ethanol. The use of cellulosic nanoparticles has shown potential uses in numerous industrial domains, such as electronics, building, packing, food, energy, and medical automobile and military.
- ❖ Compared to traditional wear-resistant ceramic coating, nanostructured ceramic coatings are far more durable and machine-resistant. Lubricants and engine oils made possible by nanotechnology also dramatically minimize wear and tear, greatly extending the life of all moving parts from industrial machinery to power tools.
- ❖ Catalysis is using more and more nanoparticles to enhance chemical responses. As a result, less catalytic material is required to generate the intended outcomes while lowering pollution and saving money. Two

large applications include automobile catalysis and petroleum refinery transformers.

- ❖ Superior household products like those made with nano-engineered materials air purifiers, environmental sensors, and degreasers and stain removers filters; antimicrobial disinfectants; and specialty coatings and adhesives goods, such house paints that are stain- and dirt-resistant.

### **1.3 ZINC OXIDE NANOPARTICLE**

ZnO is one of the multifunctional inorganic particles known for its important semiconducting properties. ZnO semiconductors retain exemplary photosensitivity due to its properties such as wide band gap (3.37 eV), high intrinsic electron mobility (300 cm<sup>2</sup>/Vs), and high exciton binding energy (60 eV). Hence ZNPs have been employed as a productive photocatalyst in the breakdown of organic contaminants. ZnO has applications extended to many areas due to its non-toxicity, low-cost, excellent chemical stability, a wide range of radiation absorption, good electrical properties, and high electrochemical coupling coefficient. Also, the physicochemical stability and the ability to form in a variety of morphologies and low-cost products finds use in the applications of ZnO-based photocatalysts. Moreover, the remarkably high thermal and mechanical stability of ZnO at room temperature makes it an attractive material for potential applications in many fields including electronics, optoelectronics, laser technology, gas sensors and energy storage devices. Strong pyroelectric and piezoelectric properties are the result of wurtzite's large electromechanical coupling and lack of a center of symmetry. Hence ZnO can be efficiently used in mechanical actuators and piezoelectric sensors.

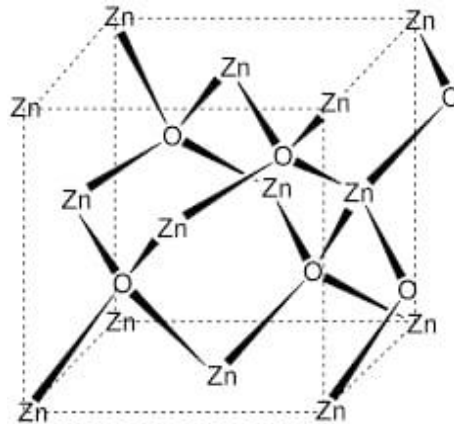


Fig 1.2 Wurtzite structure of ZnO

### 1.3.1 Uses

- ❖ ZnO is renowned for having strong UV absorption capabilities. This is widely used in cosmetics and other personal care items like sunscreen<sup>6</sup>.
- ❖ ZNPs exhibit remarkable luminescent characteristics, making them an important component of bio imaging<sup>7</sup>.
- ❖ The textile industry is drawn to ZNPs because, they have the ability to withstand bacteria, UV and visible light, and have a deodorizing effect.
- ❖ Zinc is known to maintain the structural integrity of insulin. As a result, zinc oxide nanoparticles are successfully used in the treatment of diabetes.
- ❖ Zinc is an essential element present in all body tissues and various enzymes in trace amount. Moreover, it plays an important role in protein and nucleic acid synthesis neurogenesis etc. Therefore, Nano zinc oxide is used as a food additive as nano Zn are more easily absorbed by the body.
- ❖ Drug delivery is one of the many biomedical uses for ZNPs. When it comes to drug carriers, zinc oxide is superior to other metal oxides.
- ❖ In rubber, ZNPs are added as an additive and the process of vulcanization is promoted, which is used for the manufacturing of tire.

When the tires make Churning motion, heat generates from it, but the good conductivity of ZnO nanoparticles improves the removal of generated heat to a greater extent.

### **1.3.2 Green synthesis**

<sup>8</sup>Since they produce unique phytochemicals, plant parts such as leaves, stems, roots, fruits, and seeds have been employed for the manufacture of ZnO nanoparticles. Utilizing inexpensive, environmentally acceptable plant extracts eliminates the need for intermediate base groups and is a very cost-effective approach. It produces an extremely pure, quantity-enriched product free of contaminants in a very short amount of time and without the need for expensive equipment or precursors. As they can produce stable, diversely shaped and sized NPs on a vast scale, plants are the most desired source of NP synthesis. The process of bio-reduction entails utilizing phytochemicals such as polysaccharides, polyphenolic compounds, vitamins, amino acids, alkaloids, and terpenoids secreted from the plant to reduce metal ions or metal oxides to zero valence metal NPs.

The most often used technique for making ZNPs from leaves or flowers is to thoroughly wash the plant material under running tap water and then disinfect it with double distilled water. The plant portion is then allowed to dry at room temperature before being weighed and crushed with a crusher and pestle. The plant portion is mixed with Milli-Q H<sub>2</sub>O to the appropriate concentration, and the mixture is continuously stirred with a magnetic stirrer while it boils. Whatman filter paper is used to filter the solution, and the clear solution that results is used as a plant extract. To ensure effective mixing, a certain amount of the extract is combined with 0.5 millimeter of hydrated zinc nitrate, oxide, or sulfate. The combination is then boiled at the appropriate temperature and duration. At this stage, some optimize by

varying the temperature, pH, extract concentration, and duration. The mixture becomes yellow during the incubation time, providing visual evidence that the NPs were generated. The synthesis of NPs is then verified using UV-Vis spectrophotometry. The mixture is then centrifuged, and the pellet is dried in a hot air oven to produce crystal NPS. Further, synthesized nanoparticles are characterized using X-ray diffractometer (XRD), Energy Dispersion Analysis of X-ray (EDAX), Fourier Transform Infrared Spectroscopy (FTIR), Scanning Electron Microscopy (SEM), Transmission Electron Microscopy (TEM), Field Emission Scanning Electron Microscopy (FE-SEM), Atomic Force Microscopy (AFM), Thermogravimetric Differential Thermal Analysis (TG-DTA), Photoluminescence Analysis (PL), X-ray Photoelectron Microscopy (XPS), Raman Spectroscopy, Attenuated Total Reflection (ATR), UV-Visible Diffuse Reflectance Spectroscopy (UV-DRS), and Dynamic Light Scattering (DLS).

In a study by Jafarirad et al., the results of NPs produced using two distinct methods—conventional heating (CH) and microwave irradiation (MI)—were compared. The findings amply showed that MI produces NPs more quickly because of its high heating rate, which speeds up the reaction rate. Plants belonging to Lamiaceae family have been extensively studied like *Anisochilus carnosus*, *Plectranthus amboinicus* and *Vitex negundo* which showed NP formation of varied sizes and shapes like spherical, quasi-spherical, hexagonal, rod-shaped with agglomerates. Results clearly indicated that with the increasing concentration of a plant extract, the size of synthesized NP decreases. Results also compared the size ranges observed through different techniques like FE-SEM, TEM, XRD showed similar range values. SEM and EDAX showed similar results different from results of XRD. NPs synthesized from *Vitex negundo* leaf and flower

showed the similar size of 38.17 nm confirmed by XRD analysis calculated through Debye-Scherrer equation. Leaves of *Azadirachta indica* of Meliaceae family have been most commonly used for the synthesis of ZNP. All experiments showed NPs in similar size range confirmed by XRD and TEM analysis with spherical shape and hexagonal disc shape and Nano buds. These studies elucidated the involvement of alcohol, amide, amine, alkane, carboxylic acid and carbonate moieties in the formation of NPs confirmed through FTIR studies. Nanoparticles synthesized from fresh leaf extract as well as the leaf peel of Aloe vera belonging to Liliaceae family, showed the difference in size (NP synthesized from peel was greater in size confirmed by SEM and TEM analysis) but similar in shapes (hexagonal and spherical). NPs synthesized from extracts of *Agathosma betulina*, *Moringa oleifera*, *Pongamia pinnata*, *Plectranthus amboinicus*, *Nephelium lappaceum* and *Calatropis Gigantea* showed agglomerate formation.

#### **1.4 GRAPHENE OXIDE**

The most frequent process for producing GO is oxidation of graphite oxide. Strong oxidizers are used to treat graphite to produce graphite oxide, also known as graphitic oxide or graphitic acid. Graphite oxide is a chemical consisting of carbon, oxygen, and hydrogen in varying ratios. The graphene layer's surface is functionalized with several species of oxygenated functional groups due to the oxidation process. The first reports of GO date back to Schafhaeutl in 1840 and Brodie in 1859. The long-range conjugated network of the graphitic lattice is primarily responsible for the conductivity of graphene. Carrier mobility and carrier concentration are reduced when functionalizations break the conjugated structure and localize  $\pi$  electrons. Even if a GO has conjugated areas, the lack of percolating channels between  $sp^2$  carbon clusters prevents classical carrier transport from occurring,

which prevents long-range conductivity. Synthesized GO sheets or films therefore have a sheet resistance of at least  $10^{12} \text{ ohm}^{-2}$  and are generally insulating. Improved hydrophilicity and improved layer separation are provided by the many functional groups. Because of its hydrophilicity, GO can be subjected to ultrasonic irradiation, resulting in the formation of one or more extremely stable graphene layers that can be distributed in DI water and other solvents. GO has a lot of appealing qualities. It spreads readily across a wide range of media, including different matrices, organic and aqueous solvents. The presence of both electron rich oxygen species and an electron rich graphene backbone allow for further surface functionalizations, which give rise to an adaptable material for multiple applications. GO does however, suffer from a low electrical conductivity and is an electrical insulator. GO is also soluble in many solvents, both aqueous and organic. To gain the benefits of GO it is typically dispersed, added into a formulation, made into a film or other nano-enabled product and then reduced to restore the graphene structure<sup>9</sup>.

#### **1.4.1 Structure**

Tetrahedrally bound  $\text{sp}^3$  carbon atoms, which are positioned slightly above or below the graphene plane, make up a portion of the extensively decorated graphene oxide (GO) sheets. Due to the structure deformation and presence of covalently bonded functional groups, GO sheets are atomically rough. The Scanning Transmission Electron Microscope (STEM) shows that the degree of oxidation fluctuates the nanometer scale, suggesting the presence of  $\text{sp}^2$  and  $\text{sp}^3$  carbon clusters of a few nanometers. The graphene like honeycomb lattice is preserved in GO, albeit with disorder, that is, the carbon atom attached to functional groups are slightly displaced but the overall size of the unit cell in GO remains to be that of graphene. Therefore, GO can be defined as a randomly distributed mixture of non-oxidized

regions where the majority of the carbon atoms maintain  $sp^2$  hybridization and oxidized areas with oxygen containing functional groups.

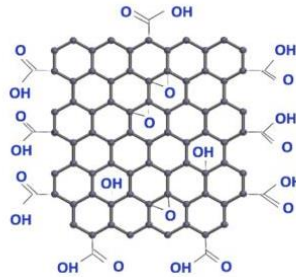


*Fig 1.3 Graphene oxide*

#### **1.4.2 Properties**

##### ❖ Mechanical strength

The ability of graphene oxide (GO) to tolerate mechanical stress and deformation is referred to as its mechanical strength. Because of its two-dimensional hexagonal lattice structure, which is resistant to bending and stretching forces, GO has good mechanical strength. Because of this characteristic, GO is appropriate for a wide range of uses, such as nanotechnology and reinforcing materials in composites.

##### ❖ Electrical conductivity

The electrical conductivity of graphene oxide differs significantly from that of graphene in its purest form. Because graphene oxide's surface contains functional groups that contain oxygen (epoxy, hydroxyl, and carboxyl), it functions better as an insulator or semiconductor than a good conductor. These groups cause the graphene lattice's structure to break, resulting in the introduction of electron scattering sites and bandgap-like characteristics. Low electrical conductivity is the result of this substantial obstruction to the flow of electric current.

Nonetheless, the electrical conductivity of graphene oxide can be increased by reduction techniques like chemical reduction or thermal treatment that eliminate some of these oxygen groups. Consequently, reduced graphene oxide (rGO) approaches the remarkable electrical properties of pristine graphene and shows improved conductivity. Because of its tunability, graphene oxide and its derivatives find use in a variety of products, such as electrical components, sensors, and energy storage devices.

❖ **Optical property**

Another distinctive and intriguing feature of graphene is its relatively high 2.3% absorption of white light, especially in light of its one atom thickness. This is because of the electrical characteristics mentioned earlier; the electrons functioning as extremely mobile, massless charge carriers.

**1.4.3 Uses**

- ❖ **Composite Materials:** The mechanical and electrical properties of composite materials can be improved by adding graphene oxide. Materials such as ceramics and polymers can have their strength and conductivity increased by it.
- ❖ **Sensing devices:** Graphene oxide-based sensors find application in gas, chemical, and biosensing fields. Graphene oxide is useful for detecting a wide range of substances due to its high surface area and reactivity.
- ❖ **Biomedical Applications:** Tissue engineering, drug delivery, and bioimaging all make use of graphene oxide. Targeted drug delivery can benefit from its biocompatibility and capacity to load drugs onto its surface.
- ❖ **Graphene oxide membranes** are employed in the desalination, gas separation, and water purification processes. Their superior barrier qualities and elevated permeability render them perfect for use in filtration processes.

- ❖ **Energy Storage:** The use of graphene oxide in batteries and supercapacitors is being investigated. It can extend these device's cycle life and capacitance.
- ❖ **Coatings:** To improve a surface's ability to withstand corrosion, wear, and ultraviolet radiation, graphene oxide can be applied as a coating material.
- ❖ **Printed Electronics:** Flexible electronics, RFID tags, and conductive patterns can be printed on a variety of substrates using graphene oxide ink.
- ❖ **Flexible Electronics:** Graphene oxide's thin, flexible nature makes it suitable for use in transparent, flexible electronics, including touch screens and flexible displays.
- ❖ **Catalysis:** Materials based on graphene oxide can act as catalysts in a variety of chemical reactions, such as the oxidation and splitting of water.
- ❖ **Environmental Remediation:** Because graphene oxide has a high adsorption capacity for heavy metals and organic compounds, it is used in the removal of pollutants from air and water.
- ❖ **Paints and Coatings:** The barrier, UV resistance, and conductivity of paints and coatings can all be enhanced by the addition of graphene oxide.
- ❖ **Nanocomposites:** By adding graphene oxide reinforcement, these materials—which include polymers, ceramics, and concrete—can exhibit better qualities.

These uses demonstrate graphene oxide's adaptability to a variety of sectors, such as electronics, materials science, energy, healthcare, and environmental technology. Research and development are still ongoing to uncover new applications for this extraordinary material.

#### **1.4.4 Synthesis**

##### **Hummer's & Modified Hummer's method:**

Brodie was the first to demonstrate the synthesis of GO. In 1859, he synthesized GO by adding a portion of potassium chlorate to a slurry of graphite in fuming nitric acid<sup>10</sup>. Later Staudenmaier changed the protocol by replacing two thirds of fuming nitric acid with concentrated sulfuric acid followed by gradual addition of chlorate to the reaction mixture<sup>11</sup>. This small modification introduced in the procedure provided a simple method for the production of highly oxidized GO. In 1958, Hummers reported an alternative method for the synthesis of graphene oxide by using  $\text{KMnO}_4$  and  $\text{NaNO}_3$  in concentrated  $\text{H}_2\text{SO}_4$ . Later Hummers method turned out to be a widely accepted and applied method for the synthesis of GO<sup>12</sup>.

The Hummers method proved to be efficient as the reaction was completed within few hours. Moreover,  $\text{KClO}_3$  was replaced by  $\text{KMnO}_4$  which greatly reduced the risk of explosion due to  $\text{ClO}_2$  and the formation of acid fog was completely removed by the use of  $\text{NaNO}_3$ .

Even though Hummers method was way better than other approaches, the oxidation process released toxic gases such as  $\text{NO}_2$  and  $\text{N}_2\text{O}_4$ . The residual  $\text{Na}^+$  and  $\text{NO}_3^-$  ions formed from  $\text{NaNO}_3$  were difficult to be removed from the waste water formed from the processes of synthesizing GO. So by excluding the use of  $\text{NaNO}_3$ , the Hummers method was modified by increasing the amount of  $\text{KMnO}_4$  at the same time to synthesize GO. In another method, the reaction was performed in a 9:1 mixture of  $\text{H}_2\text{SO}_4/\text{H}_3\text{PO}_4$  by excluding  $\text{NaNO}_3$ . This greatly helped to improve the efficiency of the oxidation process. This improved method also provided a

greater amount of hydrophilic oxidized graphene material in comparison to Hummer's method with additional  $\text{KMnO}_4$ <sup>13</sup>.

### **1.5 ZnO-GO NANOCOMPOSITE**

ZnO-GO nanocomposites are materials that consist of a combination of Zinc oxide and graphene oxide. These nanocomposites are created by incorporating ZnO nanoparticles into a matrix of graphene oxide. Combining these materials into nanocomposites can lead to enhanced or synergistic properties, making them useful in various applications.

These nanocomposites can offer advantages such as improved conductivity, increased surface area, and enhanced photocatalytic or sensing capabilities, depending on the intended application. These nanocomposites have gained attention in materials science and nanotechnology for their potential in various advanced technologies. GO has reactive hydroxyl and carboxyl groups which possess super dispersibility in solvent and this provide maximum fabrication of ZnO-GO composite.

#### **1.5.1 Properties**

- ❖ The composite of graphene oxide along with metal oxides such as ZnO display high and improved electrochemical behavior due to the redox reactions of metal oxide and conductivity as well as the larger surface area of graphene.
- ❖ The photo catalytic activity and increased stability of the ZnO-GO composite is much greater when compared to the zinc oxide as a Photocatalyst alone.
- ❖ The opto electronic properties exhibited by the ZnO-GO composite is important for its application and in the development of UV visible optoelectronic devices.

- ❖ Due to its unique properties such as good carrier mobility and largest surface area, carbonaceous materials like GO when added to ZnO shows improved UV sensing ability.

### **1.5.2 Synthesis**

The hydrothermal method uses an aqueous solution as a reaction system in a special closed vessel and allows for control over grain size, crystalline phase, particle morphology, and surface chemistry through regulation of the solution composition, reaction temperature, pressure, solvent properties, additives, and aging time, ZnO-GO nanocomposites can be prepared using this method. Additionally, it has the ability to produce nanomaterials that become unstable at high temperatures. The hydrothermal method has proved to produce nanomaterials with high vapor pressures while minimizing material loss. Furthermore, ethanol is the starting material used in this preparation due to its compatibility with the constituents, dispersion characteristics, and potential for uniform and controlled composite formation. An autoclave with a teflon lining offers good thermal insulation and helps to keep the reaction vessel's temperature constant and makes it simpler to retrieve the materials used to create the nanocomposite without them adhering to the autoclave walls.

## **1.6 PHOTOCATALYTIC ACTIVITY OF ZnO-GO COMPOSITE**

Zinc oxide is a n-type semiconductor that serves as a photo catalyst due to its wide band gap, high electron excitation binding energy and high intrinsic electron mobility. Due to its ease of preparation, relatively low cost and high catalytic activity ZnO can be used as a substitute for TiO<sub>2</sub>. Despite this the efficiency of ZnO is still low due to the factors such as its high resistivity, smooth recombination of photogenerated electron-hole pairs. In order to counter these effects and to enhance the photocatalytic activity in

the UV region, the band gap needs to be narrowed. This can be made possible by making nano composites of ZnO with compounds such as GO. When combined with GO, the recombination of electron - hole can be obstructed by acting as an electron acceptor. Moreover, due to the strong adsorption effect of GO, it can adsorb various organic dyes and thereby increase its photo degradation efficiency.

### **1.7 APPLICATIONS OF ZnO-GO COMPOSITE IN LITERATURE**

- ❖ Photocatalytic activity of ZnO-GO composite<sup>14</sup>: In literature, ZnO-GO nanocomposites prepared by precipitation method having outstanding reusability and photostability.
- ❖ In Optical properties<sup>15</sup> : ZnO-GO nanocomposites with a controlled concentration of GO hold great promise for applications in UV-Visible optoelectronic devices and large light-harvesting devices like solar cells.
- ❖ Antibacterial application<sup>16</sup> : ZNPs, RGO, ZnO-GO nanocomposites have been prepared through facile and easy sol-gel method. ZnO-GO nanocomposite exhibit better antibacterial activity than ZNPs and six standard investigated antibiotics.
- ❖ Efficient removal of Pb (II) ions<sup>17</sup> : ZnO-GO adsorbent has high affinity towards the removal of Pb (II) from the aqueous solution, making it a promising adsorbent that can be further investigated for commercial use.

## **1.8 OBJECTIVES**

- Synthesis of ZnO by green synthesis.
- Synthesis of GO by modified Hummer's method.
- Synthesis of ZnO-GO nanocomposites by hydrothermal method.
- Photocatalytic activity of nanocomposite.
- Characterization of prepared ZnO, GO and ZnO-GO nanocomposites using XRD, TEM & FTIR.

# Chapter 2

## Materials and Methods

This chapter gives a brief description of the materials and experimental procedures adopted for the present investigation.

### 2.1 MATERIALS

#### 2.1.1 Zinc nitrate

Zinc nitrate hexahydrate supplied by Nice Chemicals (P) Ltd, Kochi, Kerala was used for this study.

#### 2.1.2 Graphite powder

Graphite powder of 150 mesh, supplied by Nice Chemicals (P)Ltd, Kochi, Kerala was used.

#### 2.1.3 Hydrogen peroxide

Hydrogen peroxide supplied by Thermo Fisher Scientific India (P)Ltd, Mumbai with an assay of 30% W/V was used.

#### 2.1.4 Sulphuric acid

Sulphuric acid supplied by Nice Chemicals (P)Ltd, Kochi, Kerala with an assay of 98% W/V was used.

#### 2.1.5 Potassium permanganate

Potassium permanganate supplied by Nice Chemicals (P)Ltd, Kochi, Kerala

#### 2.1.6 Ethanol

Ethanol manufactured by Changshu Hongheng Fine Chemicals Co. Ltd, China with an assay of 99.9% W/V was used.

---

## 2.2 EXPERIMENTAL METHODS

### 2.2.1 Green synthesis of zinc oxide nanoparticles

The leaves of *Hibiscus rosa-sinensis* plant were collected locally. The leaves were washed with water and dried under sunlight. The dried leaves were grinded until it became a fine powder. The leaf extract for the reduction of zinc ions to zinc oxide nanoparticles was prepared by taking 7.5 g of finely powdered leaves in 250 ml glass beaker along with 150 ml of distilled water. The mixture was then boiled at 70 °C for 1 hour on a magnetic stirrer until the color of the solution turns light yellow. The extract was cooled to room temperature and filtered using a piece of clean cotton cloth. 50 ml of this extract was taken in a beaker and boiled to 60 °C – 80 °C using a magnetic stirrer. 5 g of zinc nitrate was added to the solution as the temperature reached 60 °C. This mixture is then boiled for 45 minutes so that it reduced to a deep yellow colored paste. This paste was then collected in a ceramic crucible and heated in a muffle furnace at 400°C for 1hour. A white colored powder was finally obtained and this was carefully collected and packed<sup>18</sup>.



*Fig 2.1 Prepared zinc oxide nanoparticles*

---

### 2.2.2 Synthesis of graphene oxide nanoparticle

GO was prepared by modified Hummer's method. About 1g of Graphite powder was added to 100 ml of 98 %  $\text{H}_2\text{SO}_4$  taken in a beaker. It was stirred for 12 hours at room temperature. The reaction mixture was then allowed to cool down to 10 °C and 4 g of  $\text{KMnO}_4$  was added very slowly. The mixture was continuously stirred for 2.5 hours while maintaining the temperature below 10 °C. Then it was diluted with 50 ml of distilled water and stirred for 1 hour. The reaction was then terminated by adding 150 ml of distilled water and 10 ml of 30 %  $\text{H}_2\text{O}_2$ . The reaction mixture was again stirred for 5 minutes at room temperature. The reaction mixture after cooling was poured into a 1 L beaker. Sufficient amount of distilled water was added to this beaker so that the precipitate could settle well. After settling, the decantation process was repeatedly done until the solution showed neutral pH. The precipitate obtained was then filtered and dried at 100 °C in a muffle furnace for 6 hours. Hence the GO nanoparticles were synthesized<sup>19</sup>.



*Fig 2.2 Prepared Graphene oxide*

### 2.2.3 Synthesis of ZnO-GO nanocomposite

ZnO-GO nanocomposite was synthesized using the hydrothermal method. The previously prepared ZnO and GO nanoparticles along with ethanol were used as the starting materials for the synthesis of the ZnO-GO nanocomposites. First, 10 mg of the obtained GO powder was dispersed in 10 mL of ethanol and 200 mg of ZnO was dispersed in 20 mL of ethanol.

---

These two solutions were then mixed homogeneously using an ultrasonic bath for 1 hour at room temperature (27 °C). The mixture was then transferred into a 100 mL Teflon-lined autoclave and was treated at 180 °C for 24 hrs. The final products were centrifuged, washed with ethanol and distilled water, and then dried at 60 °C for 12 hrs in a hot air oven to obtain ZnO-GO nanocomposites<sup>20</sup>.



*Fig 2.3 Prepared ZnO-GO nanocomposite*

#### **2.2.4 Photodegradation of Methylene Blue**

For the study of photodegradation, a methylene blue solution was prepared by adding 10 mg of dye to 1 litre of distilled water. 200 ml of this solution was transferred equally into two clean 250 ml beakers. About 20 mg of the synthesized ZnO-GO composite was added to one of the beakers and stirred well. The other one was kept blank to study the degradation of MB alone. These dispersions were kept under the exposure of sunlight. At regular intervals, the absorbance of solutions was measured using UV- Vis spectrophotometer<sup>21</sup>.

---

## 2.3 CHARACTERIZATION

### 2.3.1 X-Ray Diffraction (XRD)

X-Ray Diffraction (XRD) is used to analyze the crystal structure in the material. It provides useful information on the crystal phase, lattice constant, and average particle size of nanoparticles. X-ray diffraction is based on constructive interference of monochromatic X-rays and a crystalline sample as powder or single crystal. The monochromatic X-rays of known wavelength are generated by a cathode ray tube, filtered to produce monochromatic radiation, collimated to concentrate, and directed towards the sample.

When a monochromatic x-ray is incident on a crystal, the atomic electrons in the crystal are set into vibration and are accelerated. Following their acceleration, these electrons release radiation in all directions at a frequency equal to the incident x-rays. If the wavelength of incident radiation is large compared to the dimensions of the crystal, then the radiated X-ray are in phase with each. But since the atomic dimension are nearly equal to the wavelength of X-Ray, the radiation emitted by the electrons is out of phase with each other. These radiations may interfere constructively or destructively producing a diffraction pattern (i.e., maxima and minima) in certain directions. The phenomenon can be analyzed by the Bragg's equation,

$$2d_{hkl} \sin \theta = n\lambda$$

where  $n$  is diffraction order (1, 2, 3, and so on),  $d$  is the distance between lattice planes of atoms in the crystal,  $\theta$  is the diffraction angle, and  $\lambda$  is the wavelength of the X-rays used.

The resulting diffractogram pattern is in the form of a row of diffraction peaks reaction with relative intensity varying along with a certain value of  $2\theta$ . The number of atoms or ions and their distribution within the material's

unit cell determine the relative strength of the peak series. The diffraction pattern obtained is characteristic of the crystalline substance under investigation. Hence the method provides excellent information regarding the lattice type under investigation and its unit cell dimensions.

### **2.3.2 Fourier Transform Infrared (FTIR) Spectroscopy**

When nanoparticles are characterized, Fourier-transform infrared spectroscopy (FTIR) can reveal important details about the surface functional groups and chemical makeup of the particles. What to anticipate from an FTIR examination of nanoparticles is:

**Functional Group Identification:** FTIR is capable of identifying particular functional groups, such as hydroxyl, carboxyl, or amine groups, on the surface of nanoparticles. **Chemical composition:** It aids in figuring out the chemical makeup and verifies if particular molecules or coatings are present on the nanoparticle. **Surface Modifications:** Successful functionalization can be determined by FTIR by detecting any alterations in the nanoparticle surface brought about by coatings or modifications. **Interactions:** It sheds light on how stabilizers, surfactants, and other compounds interact with nanoparticles. **Purity:** By detecting any undesirable or impurity-containing chemicals, FTIR can also be used to evaluate the purity of produced nanoparticles. All things considered, FTIR analysis provides a thorough grasp of surface chemistry, functionalization, and interactions in nanoparticle characterization, helping to optimize synthesis procedures and applications.

By measuring the absorption of infrared radiation, Fourier-transform infrared spectroscopy (FTIR), a potent analytical method, can be used to identify chemical bonds in a sample. An infrared light beam is sent through a sample in FTIR spectroscopy, and the amount of light absorbed at each wavelength is noted. The molecular makeup of the sample allows it to

absorb particular infrared wavelengths, creating a distinct spectrum that acts as a material fingerprint. Researchers can identify new substances and ascertain the functional groups present in the material by comparing this spectrum with reference spectra. FTIR is widely used for qualitative and quantitative analysis as well as the study of molecular vibrations and interactions in a variety of domains, including chemistry, pharmacology, forensic science, and materials research.

### **2.3.3 Transmission Electron Microscopy (TEM)**

The transmission electron microscope is used in cancer research, virology, material science, pollution control, nanoparticles, nanotubes and semi conductors for research. It's a kind of microscopy where an electron beam passes through a sample to create an image. Most frequently, the specimen is a suspension on a grid or an ultrathin section that is less than 100 nm thick. When the beam passes through the sample and interacts with the electrons, an image is created.

After that, the image is enlarged and focused onto an imaging device, which could be a direct electron detector, a fluorescent screen, a layer of photographic film, or a scintillator connected to a charge-coupled device. The installed model - JEM -2100 is having a resolution of 0.24nm and acceleration voltage of 200 kv and it use LaB6 electron gun. TEMs generate higher-resolution images, provide atomic and crystallographic data, produce 2D images that are easier to interpret than 3D SEM images, and allow users to examine additional characteristics of a given sample.

### **2.3.4 UV-Visible Spectroscopy**

Measurements of the ultraviolet/visible area (UV-Vis) range in wavelength from about 200 nm to 800 nm. Transitions between a molecule's electrical energy levels occur when it absorbs ultraviolet or visible radiation. Characterization can be done with various materials' optical and electronic

properties, including films, powders, liquids, and monolithic solids. An inexpensive, straightforward, adaptable, non-destructive analytical method that works with a wide range of organic molecules and some inorganic species is UV-vis spectroscopy. UV-vis spectrophotometers measure the absorption or transmission of light through a medium as a function of wavelength.

UV-vis detectors are used in high performance liquid chromatography and ultra-high performance liquid chromatography to classify and measure the concentration of substances in liquid streams. It combines these methods with mass spectrometry to enable the detection of all animals. The radiation emitted by typical hot solids has multiple wavelengths and is mainly dependent on the solid's temperature. The energy released at each wavelength can be predicted based on the principle of chance.

UV-visible (UV-Vis) spectra are obtained when incident radiation interacts with the electron cloud in a chromophore, causing an electronic transition that involves the promotion of one or more outer shell electrons or the bonding of electrons from a ground state into a higher energy state. Substances usually have large visible and UV spectral bands .and might not demonstrate a high level of accuracy in compound recognition. However, they serve as a useful backup method of substance detection and are adequate for quantitative assays.

# Chapter 3

## Results and discussion

### 3.1 Characterization of Zinc Oxide

#### 3.1.1 XRD

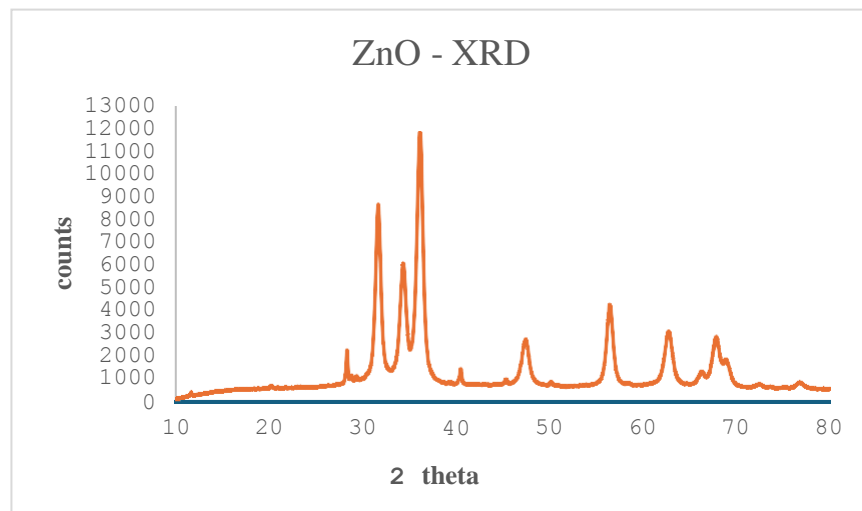


*Fig 3.1 XRD diagram of ZnO*

The XRD of the synthesized ZNPs is given in figure 3.1. The pattern clearly indicates the crystalline structure of the synthesized nanoparticles. The sharp diffraction peaks were observed at  $2\theta$  values 31.689, 34.360, 36.169, 47.465, 56.500, 62.789 & 67.842 degrees. These peaks are indexed as (100), (002), (101), (102), (110), (103) & (112) diffraction lattice planes respectively which confirm the hexagonal wurtzite structure for the synthesized nanoparticles. This pattern is in accordance with the standard peaks displayed by the International Centre for Diffraction Data. The

average size of ZNPs was calculated from the highest intense peak (101) using the Debye–Scherrer equation, where  $\lambda$  is the X-ray wavelength coming from Cu-K $\alpha$  (1.54060 Å),  $\beta$  is the full width at half maxima of the diffraction peak in radians,  $\theta$  is the Bragg's angle in degrees, and K is the shape factor and its value is equal to 0.9.

$$D = \frac{K \times \lambda}{\beta \cos \theta}$$

### **Peak 1**

$$2\theta = 31.689^\circ$$

$$\theta = 15.8445 = 0.2765 \text{ radian}$$

$$\cos \theta = 0.9999$$

$$\beta = 0.547 = 0.0095 \text{ radian}$$

$$\lambda = 1.5406 \times 10^{-10} \text{ m}$$

From Debye Scherrer Equation,

$$\begin{aligned} D_1 &= \frac{0.9 \times 1.5406 \times 10^{-10} \text{ m}}{0.0095 \times 0.9999} \\ &= \underline{14.5966 \times 10^{-9} \text{ m}} \end{aligned}$$

### **Peak 2**

$$2\theta = 34.360^\circ$$

$$\theta = 17.18 = 0.2998 \text{ radian}$$

$$\cos \theta = 0.9999$$

$$\beta = 0.648 = 0.0113 \text{ radian}$$

$$\lambda = 1.5406 \times 10^{-10} \text{ m}$$

From Debye Scherrer Equation,

$$\begin{aligned} D_2 &= \frac{0.9 \times 1.5406 \times 10^{-10} \text{ m}}{0.0113 \times 0.9999} \\ &= \underline{12.2715 \times 10^{-9} \text{ m}} \end{aligned}$$

### **Peak 3**

$$2\theta = 36.169^\circ$$

$$\theta = 18.0845 = 0.1356 \text{ radian}$$

$$\cos \theta = 0.9999$$

$$\beta = 0.683 = 0.0119 \text{ radian}$$

$$\lambda = 1.5406 \times 10^{-10} \text{m}$$

From Debye Scherrer Equation,

$$\begin{aligned} D_3 &= \frac{0.9 \times 1.5406 \times 10^{-10} \text{m}}{0.0119 \times 0.9999} \\ &= \underline{11.6528 \times 10^{-9} \text{m}} \end{aligned}$$

#### **Peak 4**

$$2\theta = 47.465^\circ$$

$$\theta = 23.7325 = 0.4142 \text{ radian}$$

$$\cos \theta = 0.9999$$

$$\beta = 0.831 = 0.0145 \text{ radian}$$

$$\lambda = 1.5406 \times 10^{-10} \text{m}$$

From Debye Scherrer Equation,

$$\begin{aligned} D_4 &= \frac{0.9 \times 1.5406 \times 10^{-10} \text{m}}{0.0145 \times 0.9999} \\ &= \underline{9.5633 \times 10^{-9} \text{m}} \end{aligned}$$

#### **Peak 5**

$$2\theta = 56.500^\circ$$

$$\theta = 28.25 = 0.4931 \text{ radian}$$

$$\cos \theta = 0.9999$$

$$\beta = 0.747 = 0.0130 \text{ radian}$$

$$\lambda = 1.5406 \times 10^{-10} \text{m}$$

From Debye Scherrer Equation,

$$\begin{aligned} D_5 &= \frac{0.9 \times 1.5406 \times 10^{-10} \text{m}}{0.0130 \times 0.9999} \\ &= \underline{10.6668 \times 10^{-9} \text{m}} \end{aligned}$$

**Peak 6**

$$2\theta = 62.789^\circ$$

$$\theta = 31.3945 = 0.5479 \text{ radian}$$

$$\text{Cos } \theta = 0.9999$$

$$\beta = 0.89 = 0.0155 \text{ radian}$$

$$\lambda = 1.5406 \times 10^{-10} \text{m}$$

From Debye Scherrer Equation,

$$\begin{aligned} D_6 &= \frac{0.9 \times 1.5406 \times 10^{-10} \text{m}}{0.0155 \times 0.9999} \\ &= \underline{\underline{8.9463 \times 10^{-9} \text{m}}} \end{aligned}$$

**Peak 7**

$$2\theta = 67.842^\circ$$

$$\theta = 33.921 = 0.5920 \text{ radian}$$

$$\text{Cos } \theta = 0.9999$$

$$\beta = 0.747 = 0.0130 \text{ radian}$$

$$\lambda = 1.5406 \times 10^{-10} \text{m}$$

From Debye Scherrer Equation,

$$\begin{aligned} D_7 &= \frac{0.9 \times 1.5406 \times 10^{-10} \text{m}}{0.0130 \times 0.9999} \\ &= \underline{\underline{10.6668 \times 10^{-9} \text{m}}} \end{aligned}$$

$$\text{Average Size} = \frac{14.5966+12.2715+11.6528+9.5633+10.6668+8.9463+10.6668}{7}$$

$$= \underline{\underline{11.1949 \text{ nm}}}$$

**Table 3.1 Recorded values of  $2\theta$ , d value, FWHM, particle size of XRD diffractogram**

Peaks ( $2\theta$ ) (Degree)	d values	FWHM ( $\beta$ )	Particle Size D (nm)	Average Particle Size (nm)
31.689	2.8213	0.547	14.5966	11.195
34.360	2.6079	0.648	12.2715	
36.169	2.4815	0.683	11.6528	
47.465	1.9140	0.831	9.5633	
56.500	1.6274	0.747	10.6668	
62.789	1.4787	0.890	8.9463	
67.842	1.3803	0.747	10.6668	

XRD analyses revealed the average size as 11.195 nm for nanoparticles. The particle size of the synthesized ZNPs was in close agreement with the previous findings<sup>22</sup>.

### 3.1.2 FT-IR

The FT-IR spectra of zinc oxide is given in figure 3.2.

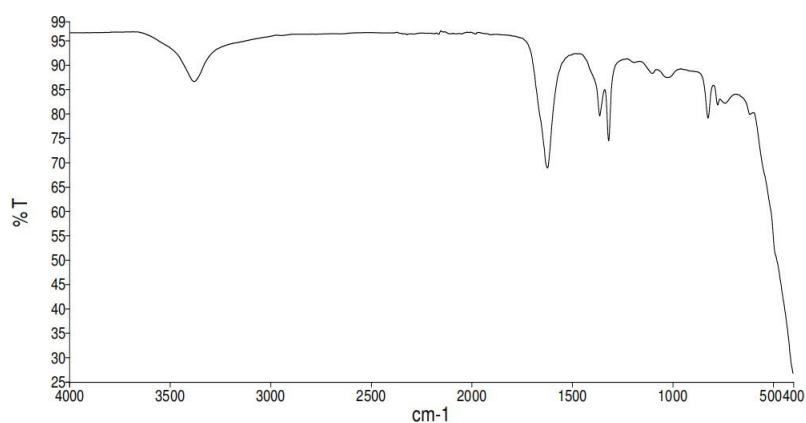


**Fig 3.2 FT-IR diagram of ZnO**

In the FTIR spectra of ZnO, a sharp and intense absorption can be seen around  $400\text{ cm}^{-1}$ . This could be due to the characteristic stretching vibration of Zn-O bond. Moreover, the peak around  $1500\text{ cm}^{-1}$  can be ascribed due to the C-C stretching vibration and an absorption around  $3400\text{ cm}^{-1}$  could be due to the stretching of O-H bond. These results are also in well accordance with the previous reports<sup>23</sup>.

### 3.1.3 HR-TEM

TEM analysis was done to understand the crystalline characteristics and size of synthesized NPs<sup>24</sup>. The images at different magnifications are shown in figure 3.3.

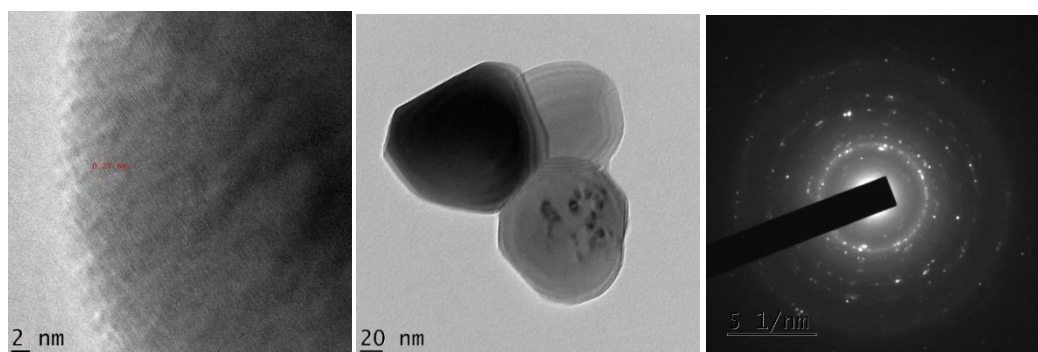


*Fig 3.3 TEM images of synthesized ZnO*

## 3.2 Characterization of Graphene Oxide (GO)

### 3.2.1 XRD

XRD analysis of the synthesized GO was done to determine the particle size, chemical composition, crystal structure, preferred orientation, and layer thickness of the prepared graphene oxide. The XRD pattern of the synthesized GO is shown in figure 3.4.

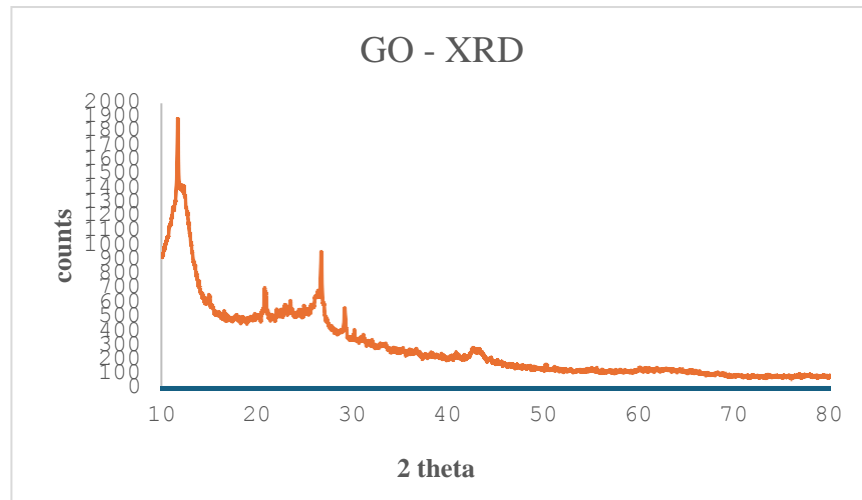


*Fig 3.4 XRD diagram of GO*

It displays the graphene oxide diffraction peaks, and we obtained three peaks at  $2\theta = 11.643^\circ$ ,  $26.683^\circ$ , and  $29.147^\circ$ , which led to the interlayer distances of 7.59434, 3.33817, and 3.06135, proving the graphene oxide's validity<sup>25</sup>. Furthermore,  $2\theta = 11.643$  shows that the peak is intense and pointed. We can determine the nanoparticles' crystalline size using these values. On applying the Debye-Scherrer equation to this, the crystalline size of nanoparticles can be calculated as

$$D = K\lambda / \beta \cos\theta$$

where  $K$  stands for the Scherrer constant (0.9),  $\lambda$  for wavelength (1.5406),  $\beta$  for the full width at half maximum (FWHM) of diffraction peaks in radians, and  $\theta$  for the Bragg angle.

### **Peak 1**

$$2\theta = 11.643^\circ$$

$$\theta = 5.8215^\circ = 0.1016 \text{ radian}$$

$$\beta = 0.142 = 0.0025 \text{ radian}$$

$$\lambda = 1.5406 \times 10^{-10} \text{ m}$$

From Debye Scherrer Equation,

$$D_1 = \frac{0.9 \times 1.5406 \times 10^{-10} m}{0.0025 \times \cos(0.1016)}$$
$$= \underline{55.4671 \text{ nm}}$$

**Peak 2**

$$2\theta = 26.683^\circ$$

$$\theta = 13.3415 = 0.2327 \text{ radian}$$

$$\beta = 0.144 = 0.0025 \text{ radian}$$

$$\lambda = 1.5406 \times 10^{-10} m$$

From Debye Scherrer Equation,

$$D_2 = \frac{0.9 \times 1.5406 \times 10^{-10} m}{0.0025 \times 0.9999}$$
$$= \underline{55.6471 \text{ nm}}$$

**Peak 3**

$$2\theta = 29.147^\circ$$

$$\theta = 14.5735 = 0.2544 \text{ radian}$$

$$\beta = 0.162 = 0.0028 \text{ radian}$$

$$\lambda = 1.5406 \times 10^{-10} m$$

$$\cos \theta = \cos(0.2544) = 0.9999$$

From Debye Scherrer Equation,

$$D_3 = \frac{0.9 \times 1.5406 \times 10^{-10} m}{0.0028 \times 0.9999}$$
$$= \underline{49.5242 \text{ nm}}$$

$$\text{Average size} = \frac{55.4671 + 55.6471 + 49.5242}{3}$$
$$= \underline{53.5461 \text{ nm}}$$

**Table 3.2 Recorded values of  $2\theta$ , d value, FWHM, particle size of XRD diffractogram**

Peaks( $2\theta$ ) (degree)	d value	FWHM ( $\beta$ )	Particle Size, D (nm)	Average Particle size (nm)
11.643	7.59434	0.142	55.4671	53.546
26.683	3.33817	0.144	55.6471	
29.147	3.06135	0.162	49.5242	

Thus, Graphene oxide has an average particle size of 53.546 nm, which guarantees that the particles are within the nanoscale. This allows us to validate that graphite can be converted into graphene oxide using a modified Hummer's method. The peaks in the XRD pattern indicate that graphene oxide is a crystalline material.

### 3.2.2 FT-IR

The FT-IR spectra of graphite and graphene oxide is given in figure 3.5 and 3.6, respectively.

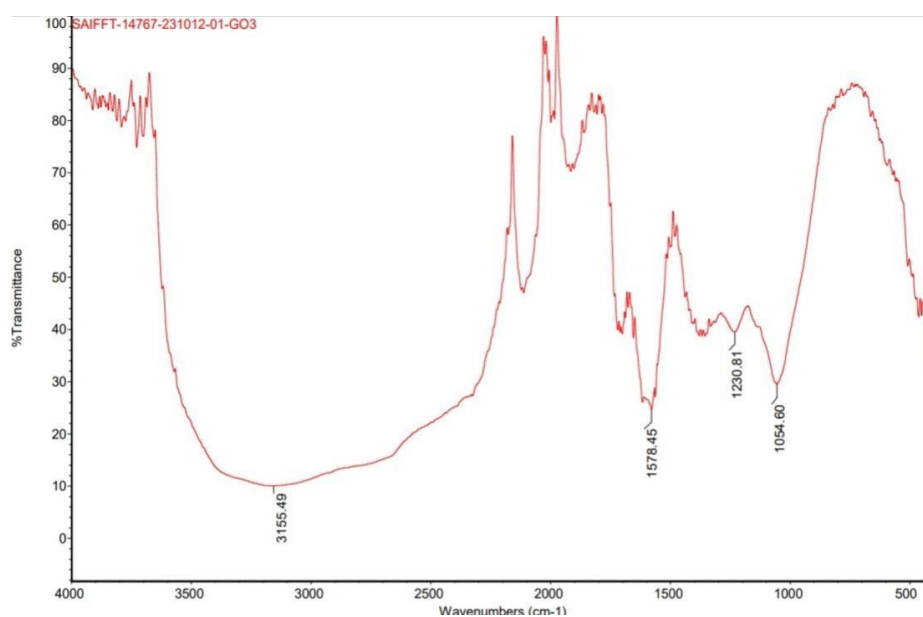


Fig 3.5 FT-IR diagram of GO

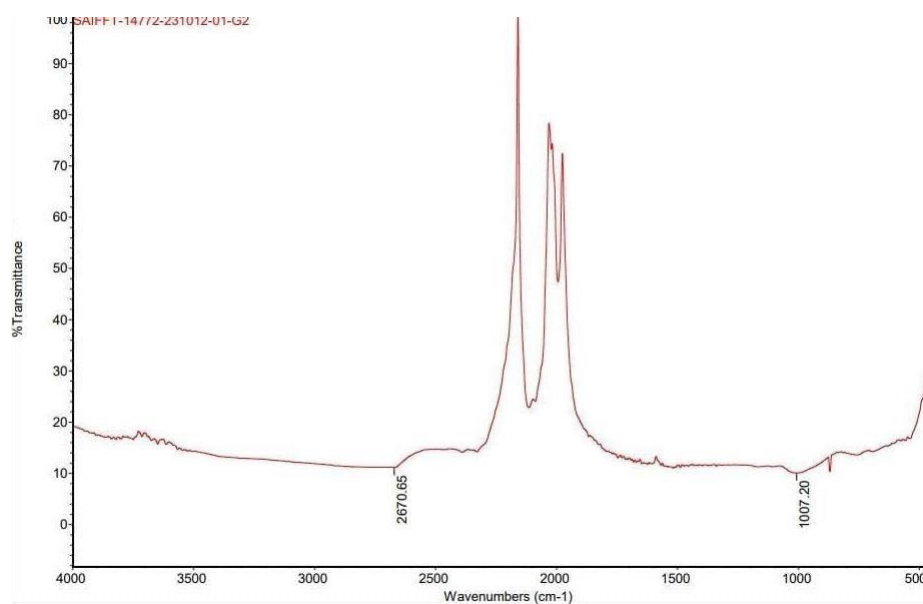


Fig 3.6 FT-IR diagram of graphite

For graphite there are no prominent peaks but in the case of Graphene oxide, there are several peaks in the spectra showing the presence of different functional groups in graphene oxide. The FT-IR spectrum shows a broad peak between the range 3000 to 3500  $\text{cm}^{-1}$ . The peaks at 3155.49  $\text{cm}^{-1}$  shows the stretching vibration of O-H groups of the water molecules adsorbed on GO<sup>26</sup>. The sharp and intense absorption around 1700  $\text{cm}^{-1}$  shows the presence of C=O group. Moreover, the absorption peak at 1578.45  $\text{cm}^{-1}$  can be attributed to the stretching vibration of C=C groups. The peaks at 1230  $\text{cm}^{-1}$  and 1054  $\text{cm}^{-1}$  shows the presence of C-OH bonds and epoxide group (C-O), respectively.

These peaks show the presence of different oxygen containing groups on graphene oxide. Hence it can be concluded that graphite has undergone oxidation to graphene oxide.

### **3.2.3 HR- TEM**

TEM analysis was done to understand the crystalline characteristics and size of synthesized NPs<sup>27</sup>. The images at different magnification are shown in Fig 3.7.

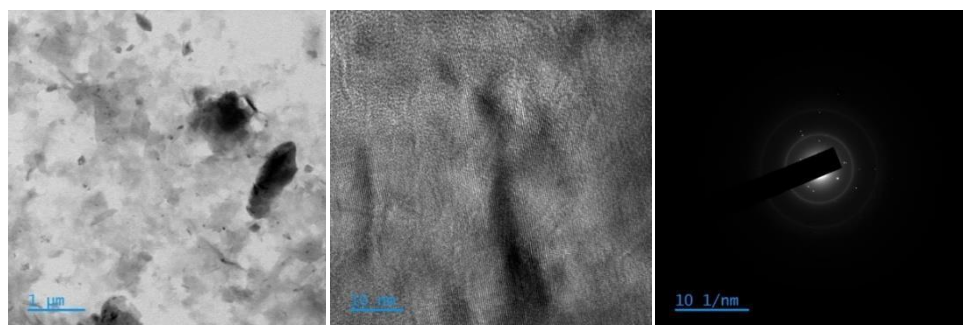


*Fig 3.7 TEM images of synthesized GO*

### 3.3 Characterization of ZnO-GO Nanocomposite

#### 3.3.1 XRD

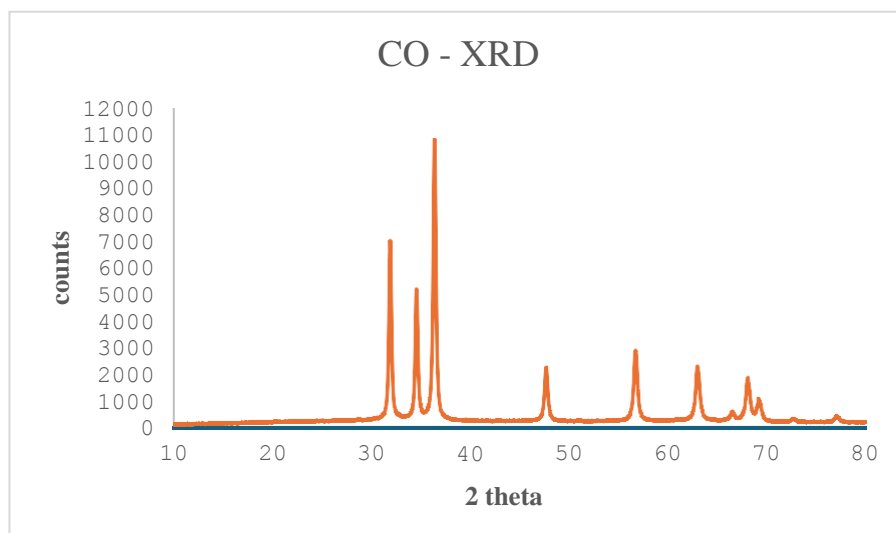


*Fig 3.8 XRD diagram of ZnO-GO nanocomposite*

Figure 3. 8 shows the XRD patterns of the ZnO-GO nanocomposite. The crystalline formation of all samples was confirmed by fitting the obtained data using the origin software. The plains of the graph matched well with the monoclinic face of zinc oxide without any observable shift in the peak position. The observed sharp and intense peaks show the highly crystalline nature of the prepared sample. The average crystalline size of pure ZnO-GO was calculated by using Debye-Scherer's Formula:  $D = k\lambda/\beta\cos\theta$ , where  $D$  is the crystalline size,  $\lambda$  is the wavelength of incident X-ray,  $\beta$  is the full width of half maximum (FWHM)of a diffraction peak,  $\theta$  is the diffraction angle and  $K$  is the Scherrer's constant. The calculated crystalline size of the prepared composite material was around 22.722 nm. The main dominant peak with height intensity (36.337) peaks of ZnO are observed in XRD

patterns of pure ZnO and ZnO-GO nanocomposites without any observable shifting.

**Peak 1**

$$2\theta = 31.853^\circ$$

$$\theta = 15.9265 = 0.2779 \text{ radian}$$

$$\text{Cos } \theta = 0.9999$$

$$\beta = 0.295 = 0.0051 \text{ radian}$$

$$\lambda = 1.5406 \times 10^{-10} \text{m}$$

From Debye Scherrer Equation,

$$\begin{aligned} D_1 &= \frac{0.9 \times 1.5406 \times 10^{-10} \text{m}}{0.9999 \times 0.0051} \\ &= \underline{\underline{27.1898 \text{ nm}}} \end{aligned}$$

**Peak 2**

$$2\theta = 34.517^\circ$$

$$\theta = 17.2585 = 0.3012 \text{ radian}$$

$$\text{Cos } \theta = 0.9999$$

$$\beta = 0.302 \text{ radian}$$

$$\lambda = 1.5406 \times 10^{-10} \text{m}$$

From Debye Scherrer Equation,

$$\begin{aligned} D_2 &= \frac{0.9 \times 1.5406 \times 10^{-10} \text{m}}{0.0053 \times 0.9999} \\ &= \underline{\underline{26.16374 \text{ nm}}} \end{aligned}$$

**Peak 3**

$$2\theta = 36.343^\circ$$

$$\theta = 18.1715 = 0.3012 \text{ radian}$$

$$2\theta = 47.639^\circ$$

$$\theta = 23.8195 = 0.1457 \text{ radian } \cos \theta = 0.9999$$

$$\beta = 0.323 = 0.0056 \text{ radian}$$

$$\lambda = 1.5406 \times 10^{-10} \text{ m}$$

From Debye Scherrer Equation,

$$D_3 = \frac{0.9 \times 1.5406 \times 10^{-10} \text{ m}}{0.0056 \times 0.9999}$$
$$= \underline{24.7621 \text{ nm}}$$

#### **Peak 4**

$$\cos \theta = 0.9999$$

$$\beta = 0.369 = 0.0064$$

$$\lambda = 1.5406 \times 10^{-10} \text{ m}$$

From Debye Scherrer Equation,

$$D_4 = \frac{0.9 \times 1.5406 \times 10^{-10} \text{ m}}{0.0064 \times 0.9999}$$
$$= \underline{21.6685 \text{ nm}}$$

#### **Peak 5**

$$2\theta = 56.689^\circ$$

$$\theta = 28.3445 = 0.4947 \text{ radian}$$

$$\cos \theta = 0.9999$$

$$\beta = 0.421 = 0.0073 \text{ radian}$$

$$\lambda = 1.5406 \times 10^{-10} \text{ m}$$

From Debye Scherrer Equation,

$$D_5 = \frac{0.9 \times 1.5406 \times 10^{-10} \text{ m}}{0.0073 \times 0.9999}$$
$$= \underline{18.9956 \text{ nm}}$$

#### **Peak 6**

$$2\theta = 62.962$$

$$\theta = 31.481 = 0.5494 \text{ radian}$$

$$\cos \theta = 0.9999$$

$$\beta = 0.452 = 0.0079 \text{ radian}$$

$$\lambda = 1.5406 \times 10^{-10} \text{ m}$$

From Debye Scherrer Equation,

$$D_6 = \frac{0.9 \times 1.5406 \times 10^{-10} \text{ m}}{0.0079 \times 0.9999}$$

$$= \underline{17.5529 \text{ nm}}$$

$$\text{Average size} = \frac{17.5529 + 18.9956 + 21.6669 + 27.1897 + 24.7621 + 26.1637}{6} = \underline{22.7218}$$

nm

**Table 3.3 Recorded values of  $2\theta$ ,  $d$  value, FWHM, particle size of XRD diffractogram**

Peaks ( $2\theta$ ) (degree)	$d$ value	FWHM ( $\beta$ )	Particle Size D (nm)	Average Particle Size (nm)
31.853	2.80715	0.295	27.1898	22.722
34.517	2.59635	0.302	26.1637	
36.343	2.47000	0.323	24.7621	
47.639	1.90738	0.369	21.6668	
56.689	1.62246	0.421	18.9956	
62.962	1.47505	0.452	17.5529	

Thus ZnO-GO Composite has an average particle size of 22.722 nm, which guarantees that the particles are within the nanoscale<sup>28</sup>. The peaks in the XRD pattern indicate that ZnO-GO Composite is a crystalline material.

### 3.3.2 FT-IR

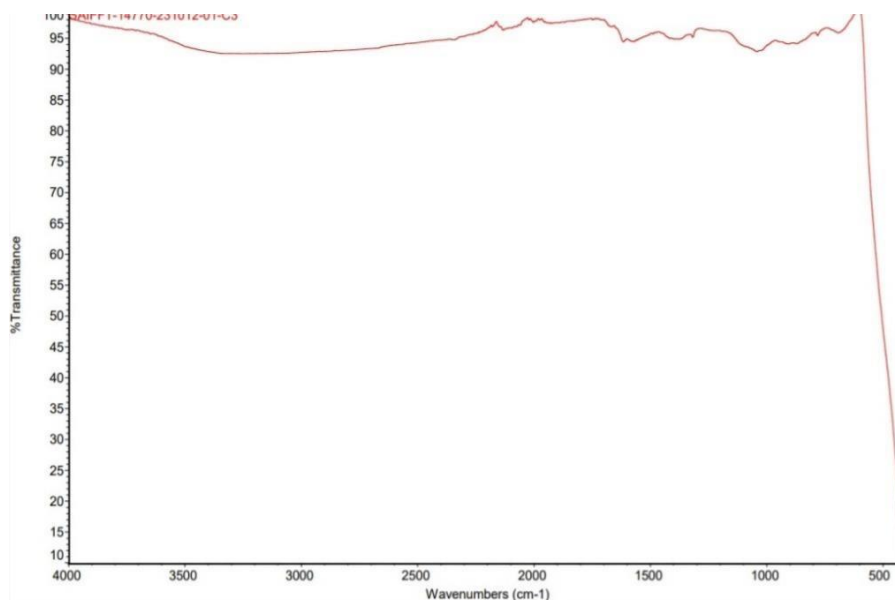


Fig 3.9 FT-IR diagram of ZnO-GO nanocomposite

From the IR spectrum of ZnO-GO nanocomposite given as figure 3.9, it can be noted that there is a sharp and intense absorption around  $400\text{ cm}^{-1}$ . This can be ascribed due to the stretching vibration of Zn-O bond<sup>29</sup>. This can confirm the presence of zinc oxide nanoparticles in the nanocomposite. Moreover, there is a marked reduction in the peak intensity of hydroxyl and epoxy groups in the spectra. All these can be attributed to the presence of ZnO on the surface of GO.

### 3.3.3 HR -TEM

TEM analysis was done to understand the crystalline characteristics and size of synthesized NPs<sup>30</sup>. The images at different magnification are shown in Fig. 3.10.

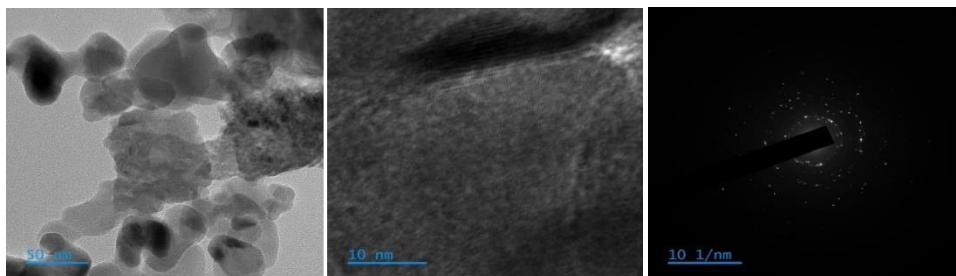
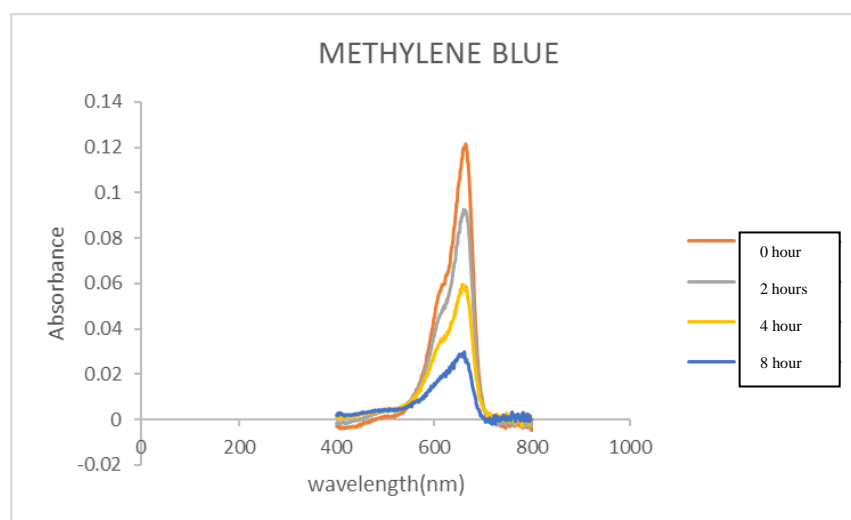
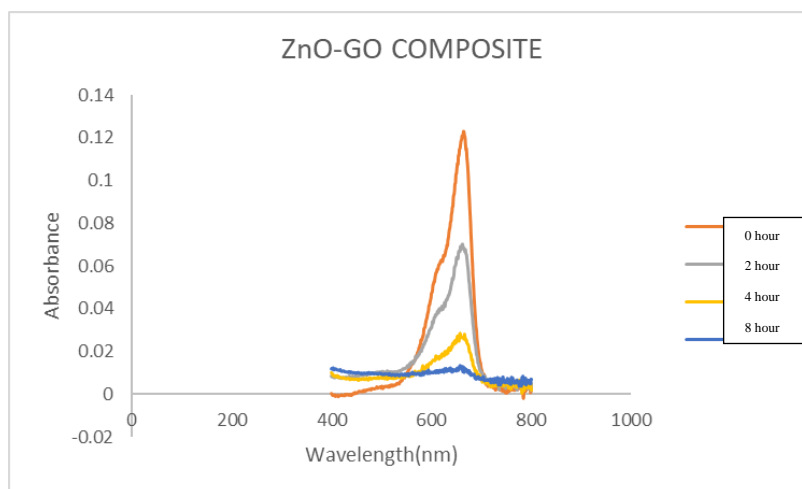


Fig 3.10 TEM images of ZnO-GO nanocomposite

### 3.4 Photo degradation of Methylene blue

#### 3.4.1 UV-Vis Spectroscopy





*Fig 3.11 UV-Vis absorption spectrum*

Figure 3.11 shows the UV-Vis spectra of MB solution before and after photo degradation. The deep blue color of the blank MB solution remained almost same throughout the time of study. Whereas, for the mixture with the composite, the deep blue color of the methylene blue solution started to fade with time.

Methylene blue shows an absorption band at 660 nm. It is clear from the graph that the absorbance of methylene blue in the blank solution decreases only slightly with time. On the other hand, the UV-Vis spectra of the dispersion of ZnO-GO composites shows a faster degradation when compared to that of the blank. After 6 hours of exposure, it can be seen that absorbance of ZnO- GO composite is much lower than the MB alone. This accounts for the improved photocatalytic activity of the composite. Thus, it can be concluded that the photo degradation of MB dye can be enhanced by using ZnO-GO nanocomposites.

# Chapter 4

## Conclusions

In this work, the ZnO-GO nanocomposites were successfully synthesized by hydrothermal method. For this, ZnO was synthesized via green routes using *Hibiscus rosa-sinensis* leaf extract and Modified Hummer's method was adopted for the preparation of GO. From the characterizations such as XRD, FT-IR, and TEM, it can be concluded that the ZnO had been successfully synthesized and the average particle size was calculated to be around 11.195 nm. The FT-IR spectra of GO showed the presence of several oxygenated functional groups which could confirm that graphite had been oxidized to GO. From the results it can be assured that ZnO had been combined with GO to form the nanocomposites with average particle size of 22.722 nm. The photodegradation of MB dye from water with the prepared nanocomposite was also studied under the influence of sunlight. We demonstrated that with the ZnO-GO nanocomposites, the degradation process was much faster than that of MB alone. Thus, the ZnO-GO nanocomposites is a potential candidate for the photocatalytic degradation of organic dyes.

## References

---

1. Patra, J. K. & Baek, K.-H. Green Nanobiotechnology: Factors Affecting Synthesis and Characterization Techniques. *J Nanomater* **2014**, 1–12 (2014).
2. Masarudin, M. J., Cutts, S. M., Evison, B. J., Phillips, Don. R. & Pigram, P. J. Factors determining the stability, size distribution, and cellular accumulation of small, monodisperse chitosan nanoparticles as candidate vectors for anticancer drug delivery: application to the passive encapsulation of [14C]-doxorubicin. *Nanotechnol Sci Appl* **67** (2015) doi:10.2147/NSA.S91785.
3. Lin, Y., Hong, R., Chen, H., Zhang, D. & Xu, J. Green Synthesis of ZnO-GO Composites for the Photocatalytic Degradation of Methylene Blue. *J Nanomater* **2020**, 1–11 (2020).
4. Ramsay, R. R., Dunford, C. & Gillman, P. K. Methylene blue and serotonin toxicity: inhibition of monoamine oxidase A (MAO A) confirms a theoretical prediction. *Br J Pharmacol* **152**, 946–951 (2007).
5. Gillman, P. K. CNS toxicity involving methylene blue: the exemplar for understanding and predicting drug interactions that precipitate serotonin toxicity. *Journal of Psychopharmacology* **25**, 429–436 (2011).
6. Ahmad Zaki, N. A., Mahmud, S. & Fairuz Omar, A. Ultraviolet Protection Properties of Commercial Sunscreens and Sunscreens Containing ZnO Nanorods. *J Phys Conf Ser* **1083**, 012012 (2018).
7. Jiang, J., Pi, J. & Cai, J. The Advancing of Zinc Oxide Nanoparticles for Biomedical Applications. *Bioinorg Chem Appl* **2018**, 1–18 (2018).

8. Agarwal, H., Venkat Kumar, S. & Rajeshkumar, S. A review on green synthesis of zinc oxide nanoparticles – An eco-friendly approach. *Resource-Efficient Technologies* **3**, 406–413 (2017).
9. T. Padmanabhan, N., Santhosh, R., Antony, A. & Mythili, U. HYDROTHERMALLY GROWN ZnO/rGO AND ZnO/PANI NANOHYBRIDS: COMPARATIVE STUDY ON THEIR ELECTRICAL CONDUCTANCE. *J Adv Sci Res* **13**, 07–11 (2022).
10. XIII. On the atomic weight of graphite. *Philos Trans R Soc Lond* **149**, 249–259 (1859).
11. Staudenmaier L. Verfahren zur Darstellung der Graphitsäure. Ber Dtsch Chem Ges; Verfahren zur Darstellung der Graphitsäure. Ber Dtsch Chem Ges 31. **31**, 1481–7 (1898).
12. Hummers, W. S. & Offeman, R. E. Preparation of Graphitic Oxide. *J Am Chem Soc* **80**, 1339–1339 (1958).
13. Marcano, D. C. *et al.* Improved Synthesis of Graphene Oxide. *ACS Nano* **4**, 4806–4814 (2010).
14. Lin, Y., Hong, R., Chen, H., Zhang, D. & Xu, J. Green Synthesis of ZnO-GO Composites for the Photocatalytic Degradation of Methylene Blue. *J Nanomater* **2020**, 1–11 (2020).
15. Kachere, A. R. *et al.* Zinc Oxide/Graphene Oxide Nanocomposites: Synthesis, Characterization and Their Optical Properties. *ES Materials & Manufacturing* (2021) doi:10.30919/esmm5f516.
16. Gingiguntla, B., Akkiniraj Chandrasekar, A. & Selvan Cruz, S. A. Green Mediated Synthesis of Zinc Oxide Nanoparticles using Tamarind Bark Extract and their Applications in Textile Dye Degradation and Antimicrobial Studies. *Asian Journal of Chemistry* **36**, 239–246 (2023).

17. Ahmad, S. Z. N. *et al.* Efficient Removal of Pb (II) from Aqueous Solution using Zinc Oxide/Graphene Oxide Composite. *IOP Conf Ser Mater Sci Eng* **736**, 052002 (2020).
18. R.Sharmila Devi<sup>À\*</sup> and R. Gayathi. green synthesis of zinc oxide nanoparticles by using hibiscus rosa-sinensis. **4**, (2014).
19. T.Padmanabhan, N., Santhosh, R., Antony, A. & Mythili, U. HYDROTHERMALLY GROWN ZnO/rGO AND ZnO/PANI NANOHYBRIDS: COMPARATIVE STUDY ON THEIR ELECTRICAL CONDUCTANCE. *J Adv Sci Res* **13**, 07–11 (2022).
20. Kachere, A. R. *et al.* Zinc Oxide/Graphene Oxide Nanocomposites: Synthesis, Characterization and Their Optical Properties. *ES Materials & Manufacturing* (2021) doi:10.30919/esmm5f516.
21. Augustine, R., Kollamparambil, N. S., M. V, K., M., U. & Chandran A., S. Silver nanoparticles: Green Synthesis using Derris trifoliata Seed Extract and It's Applications as a Sensor, Photocatalyst and Antibacterial agent. *Oriental Journal Of Chemistry* **39**, 47–55 (2023).
22. R.Sharmila Devi<sup>À\*</sup> and R. Gayathri. green synthesis of zinc oxide nanoparticles by using hibiscus rosa-sinensis .
23. Sagar Raut<sup>1</sup>, Dr. P. V. T. R. T. Green Synthesis of Zinc Oxide (ZnO) Nanoparticles Using Ocimum Tenuiflorum Leaves.
24. Chung, Y. T. *et al.* Development of polysulfone-nanohybrid membranes using ZnO-GO composite for enhanced antifouling and antibacterial control. *Desalination* **402**, 123–132 (2017).
25. Ahmad, S. Z. N. *et al.* Efficient Removal of Pb (II) from Aqueous Solution using Zinc Oxide/Graphene Oxide Composite. *IOP Conf Ser Mater Sci Eng* **736**, 052002 (2020).

- 
26. Ahmad, S. Z. N. *et al.* Efficient Removal of Pb (II) from Aqueous Solution using Zinc Oxide/Graphene Oxide Composite. *IOP Conf Ser Mater Sci Eng* **736**, 052002 (2020).
  27. Salih, E., Mekawy, M., Hassan, R. Y. A. & El-Sherbiny, I. M. Synthesis, characterization and electrochemical-sensor applications of zinc oxide/graphene oxide nanocomposite. *J Nanostructure Chem* **6**, 137–144 (2016).
  28. Ahmad, S. Z. N. *et al.* Efficient Removal of Pb (II) from Aqueous Solution using Zinc Oxide/Graphene Oxide Composite. *IOP Conf Ser Mater Sci Eng* **736**, 052002 (2020).
  29. Kachere, A. R. *et al.* Zinc Oxide/Graphene Oxide Nanocomposites: Synthesis, Characterization and Their Optical Properties. *ES Materials & Manufacturing* (2021) doi:10.30919/esmm5f516.
  30. Salih, E., Mekawy, M., Hassan, R. Y. A. & El-Sherbiny, I. M. Synthesis, characterization and electrochemical-sensor applications of zinc oxide/graphene oxide nanocomposite. *J Nanostructure Chem* **6**, 137–144 (2016).